The Impacts of Calcium Ions Substitution in Hydroxyapatite with Neodymium and Zinc on Biological Properties and Osteosarcoma Cells

Suha Q. AL-Shahrabalee[*] [iD] , **Hussein A. Jaber**

[a] Materials Engineering Dept, University of Technology-Iraq, Alsina'a Street, 10066 Baghdad, Iraq.

*Corresponding author Email: suhaqais88@gmail.com

HIGHLIGHTS

- The wet precipitation method can use to prepare valuable substituted hydroxyapatite.
- Substituted hydroxyapatite with rare earth elements (Neodymium) and Zinc have antibacterial and fungicide activity.
- Elements used in substitution can be led to a grateful change in the anticancer effect of Nd-Zn/hydroxyapatite.
- Substitute part of calcium ion with other ions can generate safe biomaterial on the human body.

ARTICLE INFO

ABSTRACT

Hydroxyapatite (HA) is one of the important biomaterials in the medical field, especially in bone treatment, because of its biological properties close to human bone. A simple co-precipitation technique was used to integrate neodymium and zinc into HA by adding neodymium nitrate and zinc nitrate as a source of substituted elements during synthesis through the wet precipitation method with controlled temperature and pH. Finally, substituted HA was sintered at 800℃ after completing the biomaterial preparation. The resulting Nd-Zn/HA was globe-like with nanoparticle size. The Ca+Nd+Zn/P ratio was equal to 1.63, which is relatively close to the molar ratio of bone. Also, the ability of Nd-Zn/HA to cause apoptosis in osteosarcoma cells was discovered. The anti-tumor actions are amplified when increasing the concentration of substituted HA. Therefore, Nd-Zn/HA is a potentially effective biomaterial in osteosarcoma treatment. Meanwhile, it has antibacterial and fungicidal properties against *Staphylococcus aureus*, *Staphylococcus epidermidis*, *Streptococcus mutans*, *Escherichia coli*, and *Candida albicans*—one of the important properties required in biomaterials to protect the part that is being treated after the biomaterial is implanted inside the body. The inhibition zone of Nd-Zn/HA ranged between (20-31)mm, much higher than gentamicin and nystatin.

1. Introduction

The biomedical field continually increases the desire for novel materials that can replace and/or repair damaged biological tissues. The majority of biomaterials used to treat musculoskeletal problems are made of calcium orthophosphates, particularly hydroxyapatite (HA), which is the inorganic phase of bone that most closely resembles bone [1], [2]. Hydroxyapatite has excellent biocompatibility [3] and is as the most common mineral in human and animal hard tissues, such as bone and tooth enamel. It is frequently utilized as a biomaterial in orthopedics [4] and maxillofacial clinical surgery to assist bone growth and remodeling. Furthermore, it is generally recognized that HA contains trace elements such as magnesium, silicon, and zinc in natural bone minerals [5]. Despite these advantages, synthetic HA has limited usage as a bone graft material due to several issues, including reaching the ideal crystallinity level, phase purity, low mechanical characteristics, and high in vitro solubility [6]. To address these issues, substantial research are being performed utilizing various ways to generate ion substituted/HA [7]. Ionic substitution has emerged as a potent strategy for improving the performance of HA, either by altering its structural, morphological, and chemical properties or by leveraging the therapeutic effects of the substituting ions [8]. In the HA crystal structure, the Ca^{2+}, PO_4^{3-}, and OH^- can all be replaced by different ions [9], where Ca^{2+} can easily be substituted by Zn^{2+}, Sr^{2+}, and Mg^{2+}; and PO_4^{3-} can easily be replaced by SiO_4^{4-} and CO_3^{2-}; and OH^- can be replaced by CO_3^{2-} and F^- [10].

Compared to pure HA, neodymium substituted hydroxyapatite (Nd/HA) with various doping levels exhibited a considerable increase in electrical conductivity, which is essential in the electromagnetic sector and for accelerating bone fracture repair. The biocompatibility test of the Nd/HA NPs on the L929 fibroblast cell line revealed that cell viability was

1

greater than 90%, with no effect on cell proliferation. Nd/HA can deliver anticancer medications with high specificity while also allowing for fluorescence imaging, which would significantly advance cancer therapy [11].

In vivo, Zn is mostly found in bone and is closely linked to bone metabolism. It enhances osteoblast proliferation and osteocalcin generation, accelerates bone matrix maturation, and suppresses osteoclast activity by stimulating bone growth and mineralization [12]. When zinc is doped into HA, it gives it a wide range of functionalities. Zn/HA has strong bioactivity, osteogenesis, antibacterial properties, and anti-inflammatory [13]. In this study, the purpose was to synthesize a new biomaterial for orthopedic application. Nd-Zn/substituted hydroxyapatite nanoparticles were prepared using the wet chemical precipitation method to study the influence of Nd and Zn insertion on the structural and biological features of the substituted hydroxyapatite with the help of different characterization techniques. In addition to studying the effect of Nd-Ce/HA on the antibacterial and fungicide activity and its effect on normal cells and osteosarcoma cells (MG63).

2. Materials and Methods

2.1 Materials and Reagents

$Ca(NO_3)_2.4H_2O$ supplied from HIMEDIA (made in India) with purity 99.9%, $Nd(NO_3)_3.6H_2O$ with purity 99.9% (SIGMA-ALDRICH, Switzerland), $Zn(NO_3)_3.6H_2O$ with purity 99.9% (HIMEDIA, India), $(NH_3)_2HPO_4$ supplied from Merck (Germany) and ammonia obtained from CHEM-LAB (Belgium) with 25% concentration.

2.2 Synthesis of Substituted Hydroxyapatite

Wet chemical precipitation is a hydroxyapatite production method involving chemical reactions between calcium and phosphorus ions at a regulated pH and temperature. (Ca + Nd + Zn) - containing solution was made by dissolving 0.167 mol of $Ca(NO_3)_2.4H_2O$, $Nd(NO_3)_3.6H_2O$, and $Zn(NO_3)_2.6H_2O$ in distilled water. In comparison, the P-containing solution was made by dissolving 0.1 mol of $(NH_3)_2HPO_4$ in distilled water, and ammonia was used to raise the pH of the P-containing solution to above 10.5. The (Ca + Nd + Zn) - containing solution was heated to 70°C. Then, the P-containing solution with constant stirring and heating was added to the (Ca + Nd + Zn) -containing solution. The reaction was carried out at 70°C for about 3 hours, and the pH of the final solution was adjusted to 11 during the chemical reaction. After completing the addition of $(NH_3)_2HPO_4$ solution, heating was turned off to allow the solution to age for one day at room temperature with a continual stirrer. The neutralization reaction is the most common reaction that produces water as a byproduct, which is then removed through filtration. To obtain Nano Nd-Zn/HA, the filtered powder was washed, dried at 100°C for several hours, sintered at 800°C, and grind.

2.3 Nd-Zn/HA Characterization Tests

2.3.1 XRD test

XRD technique was applied to verify the formation of substituted HA and their constituent in the specimens under study. (Philips X'Pert X-ray PRO, Holland) operating with CuKα radiation (λ = 1.5405 Å) was used to obtain the X-ray diffraction for Nd-Zn/HA after the preparation steps of substituted HA using the wet precipitation method. The data was drawn with a step of 0.05° point/second in 2θ between 10° and 80°. Besides that, phases were identified by comparing the peak positions of the experimental XRD patterns with those of the X'Pert HighScore Plus.

2.3.2 Fourier transform infrared spectroscopy test (FTIR)

FTIR spectroscopy was used to characterize the functional groups of Nd-Zn/HA utilizing a Bruker Tensor 27 IR, Germany (the range of spectral was from 4000 cm^{-1} to 500 cm^{-1}, standard KBr beam splitter). When the transmittance mode is used, the acquired FTIR spectra represent the entire material.

2.3.3 Field emission scanning electron microscope (FE-SEM) with energy dispersive x-ray spectroscopy (EDS)

A Field Emission Scanning Electron Microscope (FE-SEM) was used to characterize the morphology and size of the sample; moreover, an energy dispersive X-ray spectroscopy (EDS) measurement was obtained in the same equipment to confirm the existence of Ca, Nd, Zn, P, and O in the prepared substituted HA and help in the calculation of the new Ca+M/P ratio. All verification tests were done at room temperature and taken using (Zeiss Sigma 300-HV, Germany).

2.4 Biological Examinations

2.4.1 Antimicrobial activity of Nd-Zn/HA

Antibacterial and antifungal activity is one of the most important properties of hydroxyapatite. Three varieties of gram-positive bacteria (*Staphylococcus aureus*, *Staphylococcus epidermidis*, and *Streptococcus mutans*) and one type of gram-negative bacteria (*Escherichia coli*) were used to investigate the action of produced Nd-Zn/HA. In addition, the activity of substituted HA against fungi was also examined, with *Candida albicans* as the chosen fungus. Biological activity was assessed using the well diffusion method after microbes were activated in the lab under controlled conditions. Gentamicin tablets with a concentration of 10 micrograms were employed as a comparison for antibacterial action, whereas nystatin was used for the fungal activity.

2.4.2 Cytotoxicity assay of Nd-Zn/HA

Because of bone's remarkable regenerating capacity, especially in younger people, most fractures mend without requiring extensive surgery. Despite this, significant bone defects, such as those seen after bone tumor removal and severe nonunion fractures, lack the template for controlled regeneration and necessitate surgical intervention. As is well known, hydroxyapatite has many advantages that help the bone heal faster, but it lacks many other features, such as its limited resistance to cancer cells. The effect of Nd-Zn/HA on normal cell lines and cancer cells was investigated using an MTT assay on the WRL68 and MG63 cell lines, respectively. The cells were cultured and then incubated at 37°C in a CO_2 incubator. Serial dilutions were prepared for Nd-Zn/HA (6.25 µg/mL - 400 µg/mL). Each dose of substituted HA was introduced to MG63 cells, and these cultivated cells were incubated for a sufficient amount of time at 37°C in the presence of 5% CO_2. MTT solution (10µL) was injected into these wells and incubated again at 37°C with 5% CO_2. The media was removed, and a solution was added to each well to solubilize the formazan crystals. After complete incubation in a humidified atmosphere, The absorbance of the samples was measured at 575 nm using an ELISA reader (Bio-rad, Germany). The data were finalized using statistical analysis (Graph Pad Prism).

3. Results and Discussion

3.1 XRD

The XRD pattern of sintered HA is shown in Figure 1. The graph depicts the typical peaks of HA at 26.0382º, 28.2992º, 31.9124º, 34.2196º, 40.0930º, 42.2802º, 43.9806º, 46.8637º, 49.6456º, 53.4106º, and 64.1873º according to JCPDS cards number (00-001-1008), (01-074-0565), and (96-900-1234). Substituted elements were also obvious in XRD peaks in addition to HA, where the peaks 28.2992º, 29.1297º, 31.9124º, 34.2196º, 42.2802º, 43.9806º, 48.1707º, 49.6456º, 52.2604º, 60.2347º, 63.1724º, 64.1873º, 75.7173º, and 77.2430º matches the neodymium JCPDS cards number (00-039-0914), (00-052-0798), and (01-089-2922), while the peaks 75.7173º, 77.2430º were found that belongs to zinc according to JCPDS cards number (98-042-1015), (98-065-3501), and (98-065-3505). The crystal system of hydroxyapatite is hexagonal [14]. It was revealed through mathematical calculations, including the use of Miller indices and d-spacing in Table 1, that the value of the lattice parameters after substituting part of the calcium ions with neodymium and zinc was 9.63Å for a and b, while the value of parameter c was 7.9Å. By using the Scherrer equation, it was found that the average crystal size of the substituted HA was 28.3nm.
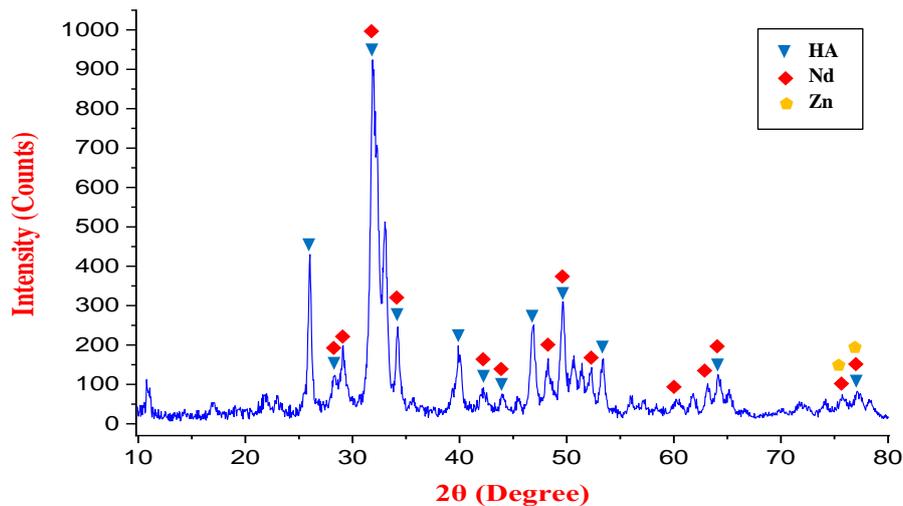

Figure 1: XRD test of Nd-Zn/HA with the explanation of HA, Nd, and Zn peaks

Table 1: Data extracted from the XRD test of Nd-Zn/HA

Peak position 2θ (°)	FWHM	Interplaner spacing d (Å)	Miller indices (hkl)
26.0382	0.2952	3.42219	002
28.2992	0.2952	3.1537	120
31.9124	0.3444	2.8044	121
34.2196	0.2460	2.62042	022
40.0930	0.4428	2.24906	221
42.2802	0.5904	2.13764	032
43.9806	0.3936	2.05885	113
46.8637	0.3444	1.93869	222
49.6456	0.2952	1.83638	123
53.4106	0.3936	1.71548	004
64.1873	0.4920	1.45103	233

3.2 FTIR Test

Figure 2 shows the FTIR spectrum of an Nd-Zn/hydroxyapatite sample generated by wet precipitation, and Table 2 lists the functional groups that have been identified. Peaks 1023.34cm⁻¹ and 1087.88cm⁻¹ were caused by asymmetrical stretching of a phosphate group (PO_4^{3-}), while band 962.65cm⁻¹ was caused by symmetric stretching, indicating the existence of hydroxyapatite that was free of organic materials. The characteristic band at 630.19cm⁻¹ was for the bending mode of a hydroxyl group (OH⁻) while the bands 1638.79cm⁻¹ and 3570.54cm⁻¹ were assigned to the stretching vibration of the (OH⁻) group [15]. The low intensity of other chemical groups can also be noticed in the FTIR test because of preparation conditions. The presence of many functional groups in addition to the essential HA groups (PO_4^{3-}, OH⁻) was because the prepared HA is made by reacting two solutions in an aqueous environment, which promotes the synthesis of a large number of functional groups in the structure of substituted HA, the most important of which is the presence of carbonate groups. Carbonate ions are replaced by hydroxyl ions (A type substitution), and carbonate ions can also be replaced by phosphate ions in this form of substituted HA (B type substitution). Thus, this functional group is beneficial because the negative charge carriers initiate and support the synthesis of bone-type apatite in the presence of the SBF. As a result, this method of substitution enhances the bioactivity of HA powder [16].

Table 2: Chemical groups of Nd-Zn/HA with their description

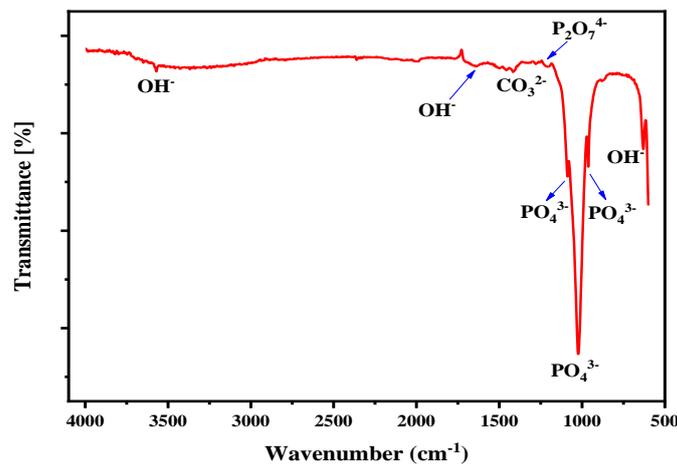| Functional groups	Wavenumber (cm⁻¹)	Description	Reference
(OH)⁻	630.19		[17]
	1638.79	Prove formation of HA	[18]
	3570.54		[19]
(PO_4)³⁻	962.65		[20]
	1023.34	Prove formation of HA	[21]
	1087.88		[16]
(CO_3)²⁻	1416.78	The low intensity of CO_3^{2-} indicates a greater assay degree	[21]
(P_2O_7)⁴⁻	1209.30	Originates when 1.5<Ca/P<1.677	[22]

Figure 2: FTIR spectroscopy of Nd-Zn/HA with the explanation of functional groups

3.3 FE-SEM and EDS

The nano-sized cluster-like particles for Nd-Zn/HA powder generated by the wet precipitation method were revealed by FE-SEM analysis as indicated in Figure 3 (a) and (b) at the magnifications of 100.00 KX and 5.00 KX with resolutions of 100nm and 2μm, respectively. Figure 3 (a) indicates the Posner cluster which belongs to the ACP structure. The pH of the solution, the concentrations of the mixing reagents, and the preparation temperature all influence the size of the ACP particles; for example, a higher supersaturation results in smaller ACP particles [23]. FE-SEM test displayed the formation of Posner clusters which are ACP structural units with a globular-like structure that have been postulated as mineralization precursors, they have a size in the nanometer range. Also, there are a lot of globular-like particles that don't seem to be nodular-type defects but could be ACP cluster agglomerates [24]. ACP is a mineral phase that forms in mineralized tissues and was the first manufactured industrial hydroxyapatite, where before that it had previously been found in the otoliths of blue sharks, as well as in chiton teeth as a precursor phase of carbonated hydroxyapatite [25]. ACP is thought to have a unique role as a bioapatite precursor and a transient stage in biomineralization [26]. Figure 4 depicts the chemical composition of Nd-Zn/substituted hydroxyapatite, which illustrates the presence of essential hydroxyapatite elements with substituted elements (Nd and Zn). The Ca/P ratio will alter after substituting Ca+Nd+Zn/P and become equal to 1.63, which is relatively close to the molar ratio of bone, as shown in the attached table. Changes in pH and sintering temperature are two important factors that influence the Ca/P ratio. [27] where Nd-Zn/HA was prepared at highly alkaline pH, and the sintering process was the step that followed the preparation process at 800°C. It is necessary to show the distribution of essential and substituted elements that compose substituted HA, which is obvious in Figure 5.
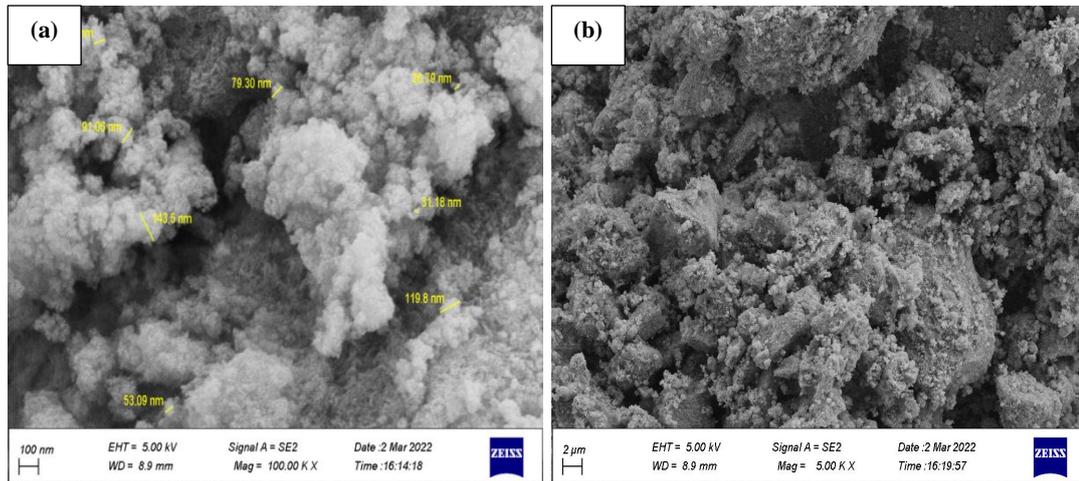
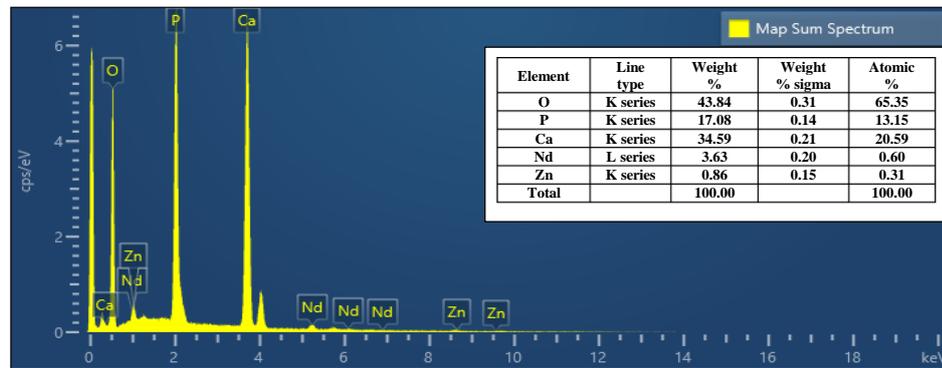**Figure 3:** FE-SEM image of (a) particle size of Nd-Zn/HA and (b) Nd-Zn/HA

Element	Line type	Weight %	Weight % sigma	Atomic %
O	K series	43.84	0.31	65.35
P	K series	17.08	0.14	13.15
Ca	K series	34.59	0.21	20.59
Nd	L series	3.63	0.20	0.60
Zn	K series	0.86	0.15	0.31
Total		100.00		100.00

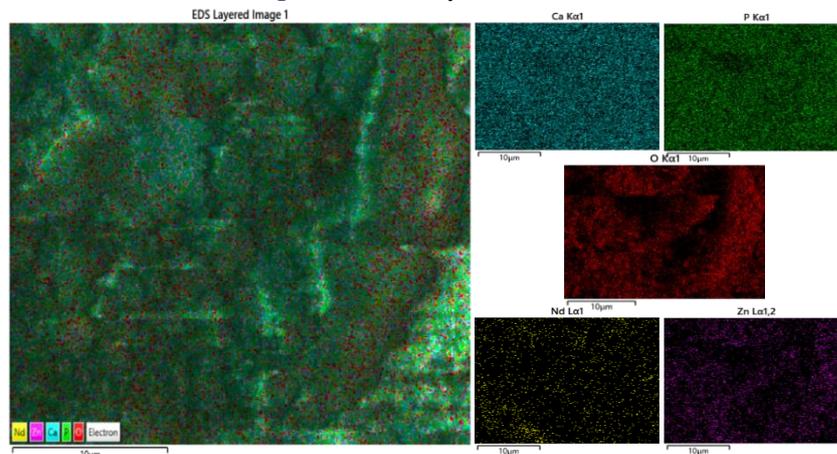**Figure 4:** EDS analysis of Nd-Zn/HA

Figure 5: EDS mapping to explain the elemental distribution of Nd-Zn/HA

3.4 Antibacterial and Fungicide Activity

Antibiotic resistance has emerged in many bacterial species, driving efforts to develop new materials with potent antibacterial properties. Implant-related bone infections are also caused by bacterial adhesion and biofilm formation. As a result, searching for new antibacterial treatments is worthwhile. Substituted HA is one of the active biomaterials for intraoperative therapy and the prevention of bone infections, where nanometer-sized HA can effectively decrease antibacterial activity [28]. It is evident from Figure 6 that Nd-Zn/HA is highly resistant to bacteria and fungi as compared to gentamicin and nystatin, respectively. The rare earth elements, including Nd, are poisonous to bacteria and fungi. Many filamentous fungal hyphae have aberrant morphological traits when rare earth elements are present, like multiple terminal branching, lateral branching, swelling, and the breaking of hyphal threads via a mechanism similar to plasmolysis. These components also prevent the development of asexual spores [29]. Regarding Zn, it was found that Zn/HA has active resistance against common human pathogens from bacteria and fungi, including *S. aureus*, *E. coli* [30], *S. mutans*, and *C. albicance* [31]. There are various facets to the mechanism by which zinc ions inhibit microbial growth where zinc ions harm the cell membranes and increase cell permeability. Furthermore, Zn interacts with the proper functioning of bacterial enzymes (like ATPase, pyruvate kinase, or
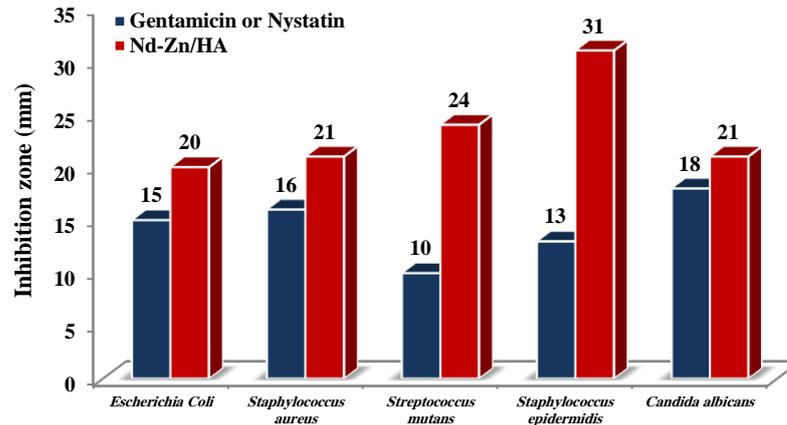
Figure 6: Antibacterial and fungicide activity of Nd-Zn/HA

glycolytic enzymes) [32]. Thus, these two substitution elements in HA structure act professionally to resist bacteria and fungi compared with the normal HA, where the antimicrobial effect of HA is much lower than the prepared substituted HA [33]. Thus, the elements neodymium and zinc, included in the composition of hydroxyapatite, work synergistically in resist bacteria and fungi.

3.5 MTT Assay

The high IC_{50} value of Nd-Zn/HA for the normal cell line (211.4 µg/mL) and the anti-tumor activity against the MG63 cell line are evident from the relationship between viability and concentration in Figure 7 and Table 3. The activity of the substituted HA against osteosarcoma cells increases with the concentration of Nd-Zn/HA. This activity reaches its peak at a 400µg/mL concentration with a 61.23±2.99% reduction in cancer cells. On the other hand, it was found that Nd-Zn/HA had a weak effect on MG63 at low concentrations (6.25, 12.5, 25, and 50 µg/mL). Still, the viability climbed to 61.61±3.97, 45.53±4.25, and 38.77±2.99 at 100, 200, and 400 µg/mL, respectively, demonstrating that Nd-Zn/HA displayed strong anticancer activity ($p < 0.0001$) against the MG63 cell line at high concentrations, with approximately safe effect on normal cells (WRL68) at all concentrations. Nd-doped HA was tested with various doping rates (1, 5, 10, and 20%), and it was safe for normal cells [34]; besides that, It can deliver anticancer drugs with great selectivity, which would be a huge step forward in cancer treatment. [35]. The anticancer properties of Nd are due to its cytotoxic agents, where the ion's increased cytotoxicity is accompanied by antioxidants, and the activity of Nd compounds could be linked to coordinative bonding. [36]. Zn is a vital element required by the human body. It has a high biocompatibility with living cells, allowing endothelium and osteoblast (OBs) cells to survive and spread, improving OBs adhesion, and increasing cell proliferation. However, it is cytocompatible with various cancer cells, including MC3T3-E1 and MG63. [37]. Zn is mostly present in human bones, and its metabolism is intimately tied to bone metabolism. It increases osteoblast proliferation, and osteocalcin synthesis speeds up bone matrix maturation and inhibits osteoclast activity. Zinc doping in HA confers several benefits, including increased bioactivity, osteogenesis potential, and anti-inflammatory characteristics. [38]. Thus, the elements of neodymium and zinc that were included in the composition of hydroxyapatite work synergistically in improving the development and growth of bones and the resistance of cancer cells.
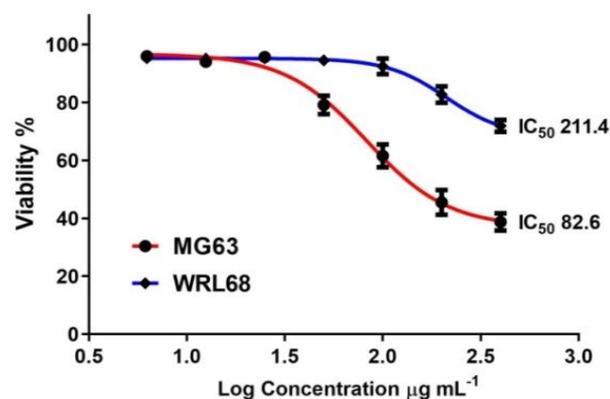

Figure 7: Relationship between viability and Log concentration
to explain the cytotoxic effect of Nd-Zn/HA on MG63
and WRL68 cell lines

Table 3: Cytotoxicity effect of Nd-Zn/HA on MG63 and WRL68 cell lines

Concentration (µg/mL)	Viability %			
	MG63		WRL68	
	Mean±SD	Specimens Number	Mean±SD	Specimens Number
6.25	95.95±0.53	3	95.29±1.5	3
12.5	94.02±0.98	3	95.18±0.41	3
25	95.72±0.81	3	95.22±0.82	3
50	79.13±3.18	3	94.56±1.10	3
100	61.61±3.97	3	92.44±2.71	3
200	45.53±4.25	3	82.75±2.84	3
400	38.77±2.99	3	71.95±2.10	3

4. Conclusion

Hydroxyapatite proved to be an essential component of biomaterials. It is widely used in dental implantology and reconstruction medicine. The wet precipitation process was used to make Nd-Zn/HA and followed by sintering at 800°C. It was characterized using XRD, FTIR, and SEM-EDS techniques, revealing the formation of substituted HA with functional groups in addition to the presence of substitute elements (Nd and Zn) in the new HA structure. The value of the Ca+Nd+Zn/P ratio was 1.63, which is close to the Ca/P ratio for bone, resulting in a considerable shift in biological characteristics. In addition, the substituted elements increased hydroxyapatite's resistance to various bacteria and fungi. It also has the value of 211.4 for IC_{50}, which means that it was safe for normal cells (WRL68) and has an anticancer effect on MG63 with the maximum capability to kill cancer cells (61.23%) at 400 µg/mL.

Author contribution

All authors contributed equally to this work.

Data availability statement

The data that support the findings of this study are available on request from the corresponding author.

Conflicts of interest

The authors declare that there is no conflict of interest.

References

[1] A. Bigi and E. Boanini, "Functionalized biomimetic calcium phosphates for bone tissue repair," *Journal of Applied Biomaterials and Functional Materials.*, 15 (2017) e313–e325.doi: 10.5301/jabfm.5000367.

[2] R. Afif and M. Anaee, "Properties of Functionally Graded Coating of Al_2O_3 /ZrO_2 /HAP on SS 316L," *Int. J. Sci. Eng. Res.*, 6 (2015) 953–957. [Online]. Available: http://www.ijser.org.

[3] R. A. Anaee, "Behavior of Ti/HA in Saliva at Different Temperatures as Restorative Materials," *J. Bio- Tribo-Corrosion.*, 2 (2016) 1–9.doi: 10.1007/s40735-016-0036-1.

[4] A. Mehatlaf, A. Atiyah, and S. Farid, "An Experimental Study of Porous Hydroxyapatite Scaffold Bioactivity in Biomedical Applications," *Eng. Technol. J.*, 39 (2021) 977–985.doi: 10.30684/etj.v39i6.2059.

[5] Y. Wang *et al.*, "Dual functional selenium-substituted hydroxyapatite," *Interface Focus.*, 2 (2012) 378–386.doi: 10.1098/rsfs.2012.0002.

[6] T. Kokubo, H. M. Kim, and M. Kawashita, "Novel bioactive materials with different mechanical properties," *Biomaterials.*, 24 (2003) 2161–2175.doi: 10.1016/S0142-9612(03)00044-9.

[7] F. Witte *et al.*, "Biodegradable magnesium-hydroxyapatite metal matrix composites," *Biomaterials.*, 28 (2007) 2163–2174.doi: 10.1016/j.biomaterials.2006.12.027.

[8] A. M. Pietak, J. W. Reid, M. J. Stott, and M. Sayer, "Silicon substitution in the calcium phosphate bioceramics," *Biomaterials.*, 28 (2007) 4023–4032.doi: 10.1016/j.biomaterials.2007.05.003.

[9] M. Safarzadeh *et al.*, "Effect of multi-ions doping on the properties of carbonated hydroxyapatite bioceramic," *Ceram. Int.*, 45 (2019) 3473–3477.doi: 10.1016/j.ceramint.2018.11.003.

[10] D. Arcos and M. Vallet-Regí, "Substituted hydroxyapatite coatings of bone implants," *Journal of Materials Chemistry B.*, 8 (2020) 1781–1800.doi: 10.1039/c9tb02710f.

[11] T. Tite *et al.*, "Cationic substitutions in hydroxyapatite: Current status of the derived biofunctional effects and their in vitro interrogation methods," *Materials (Basel).*, 11 (2018) 1–62.doi: 10.3390/ma11112081.

[12] H. Kabir, K. Munir, C. Wen, and Y. Li, "Recent research and progress of biodegradable zinc alloys and composites for biomedical applications: Biomechanical and biocorrosion perspectives," *Bioactive Materials.*, 6 (2021) 836–879.doi: 10.1016/j.bioactmat.2020.09.013.

[13] V. Chopra *et al.*, "Synthesis and Evaluation of a Zinc Eluting rGO/Hydroxyapatite Nanocomposite Optimized for Bone Augmentation," *ACS Biomater. Sci. Eng.*, 6 (2020) 6710–6725.doi: 10.1021/acsbiomaterials.0c00370.

[14] G. S. Kumar, E. K. Girija, M. Venkatesh, G. Karunakaran, E. Kolesnikov, and D. Kuznetsov, "One step method to synthesize flower-like hydroxyapatite architecture using mussel shell bio-waste as a calcium source," *Ceram. Int.*, 43 (2017) 3457–3461.doi: 10.1016/j.ceramint.2016.11.163.

[15] L. Sheikh, S. Sinha, Y. N. Singhababu, V. Verma, S. Tripathy, and S. Nayar, "Traversing the profile of biomimetically nanoengineered iron substituted hydroxyapatite: Synthesis, characterization, property evaluation, and drug release modeling," *RSC Adv.*, 8 (2018) 19389–19401.doi: 10.1039/c8ra01539b.

[16] P. Andrea *et al.*, "Comparative study between natural and synthetic Hydroxyapatite : structural , morphological and bioactivity properties," *Matéria (Rio de Janeiro).*, 23 (2018).doi: 10.1590/S1517-707620180004.0551

[17] S. Meejoo, W. Maneeprakorn, and P. Winotai, "Phase and thermal stability of nanocrystalline hydroxyapatite prepared via microwave heating," *Thermochim. Acta.*, 447 (2006) 115–120.doi: 10.1016/j.tca.2006.04.013.

[18] F. Bollino, E. Armenia, and E. Tranquillo, "Zirconia/hydroxyapatite composites synthesized via sol-gel: Influence of hydroxyapatite content and heating on their biological properties," *Materials (Basel).*, 10 (2017) 757.doi: 10.3390/ma10070757.

[19] O. Kaygili, "Structural and Dielectrical Properties of Ag- and Ba-Substituted Hydroxyapatites," *J. Inorg. Organomet. Polym. Mater.*, 24 (2014) 1001–1008.doi: 10.1007/s10904-014-0074-4.

[20] M. Andrean *et al.*, "Synthesis of hydroxyapatite by hydrothermal and microwave irradiation methods from biogenic calcium source varying pH and synthesis time," *Boletín la Soc. Española Cerámica y Vidr.*, 61 (2020) 35–41.doi: 10.1016/j.bsecv.2020.06.003.

[21] S. Ferraris *et al.*, "Acta Biomaterialia Bioactive materials : In vitro investigation of different mechanisms of hydroxyapatite precipitation," *Acta Biomater.*, 102 (2020) 468–480.doi: 10.1016/j.actbio.2019.11.024.

[22] A. Destainville, E. Champion, D. Bernache-Assollant, and E. Laborde, "Synthesis, characterization and thermal behavior of apatitic tricalcium phosphate," *Mater. Chem. Phys.*, 80 (2003) 269–277.doi: 10.1016/S0254-0584(02)00466-2.

[23] S. V. Dorozhkin, "Amorphous Calcium Orthophosphates: Nature, Chemistry and Biomedical Applications," *Int. J. Mater. Chem.*, 2 (2012) 19–46.doi: 10.5923/j.ijmc.20120201.04.

[24] K. A. Prosolov, V. V. Lastovka, O. A. Belyavskaya, D. V. Lychagin, J. Schmidt, and Y. P. Sharkeev, "Tailoring the surface morphology and the crystallinity state of cu-and zn-substituted hydroxyapatites on Ti and Mg-based alloys," *Materials (Basel).*, 13 (2020) 1–20.doi: 10.3390/ma13194449.

[25] J. Zhao, Y. Liu, W. Bin Sun, and H. Zhang, "Amorphous calcium phosphate and its application in dentistry," *Chem. Cent. J.*, 5 (2011) 40.doi: 10.1186/1752-153X-5-40.

[26] E. D. Eanes, "Amorphous Calcium Phosphate: Thermodynamic and Kinetic Considerations," in *Calcium Phosphates in Biological and Industrial Systems*, *Springer, Boston, MA.*, (1998) 21–39.doi: 10.1007/978-1-4615-5517-9_2.

[27] V. Rodríguez-Lugo *et al.*, "Wet chemical synthesis of nanocrystalline hydroxyapatite flakes: Effect of pH and sintering temperature on structural and morphological properties," *R. Soc. Open Sci.*, 5 (2018) 180962.doi: 10.1098/rsos.180962.

[28] Harun, W. S. W., R. I. M. Asri, A. B. Sulong, S. A. C. Ghani, and Z. Ghazalli. "Hydroxyapatite–Advances in Composite Nanomaterials." *Biomedical Applications and Its Technological Facets. In Tech.*, 2018.doi: 10.5772/intechopen.68820.

[29] D. E. Talburt and G. T. Johnson, "Some Effects of Rare Earth Elements and Yttrium on Microbial Growth," *Mycologia.*, 59 (1967) 492–503.doi: 10.2307/3756768.

[30] D. Predoi *et al.*, "Textural, structural and biological evaluation of hydroxyapatite doped with zinc at low concentrations," *Materials (Basel).*, 10 (2017) 229.doi: 10.3390/ma10030229.

[31] K. P. Tank, K. S. Chudasama, V. S. Thaker, and M. J. Joshi, "Pure and zinc doped nano-hydroxyapatite: Synthesis, characterization, antimicrobial and hemolytic studies," *J. Cryst. Growth.*, 401 (2014) 474-479.doi: 10.1016/j.jcrysgro.2014.01.062.

[32] A. Anwar, S. Akbar, A. Sadiqa, and M. Kazmi, "Novel continuous flow synthesis, characterization and antibacterial studies of nanoscale zinc substituted hydroxyapatite bioceramics," *Inorganica Chim. Acta.*, 453 (2016) 16–22. doi: 10.1016/j.ica.2016.07.041.

[33] S. Balu, M. V. Sundaradoss, S. Andra, and J. Jeevanandam, "Facile biogenic fabrication of hydroxyapatite nanorods using cuttlefish bone and their bactericidal and biocompatibility study," *Beilstein J. Nanotechnol.*, 11 (2020) 285–295.doi: 10.3762/bjnano.11.21.

[34] Y. Li, C. P. Ooi, P. Cheang Hong Ning, and K. Aik Khor, "Synthesis and characterization of neodymium(III) and gadolinium(III)-substituted hydroxyapatite as biomaterials," *Int. J. Appl. Ceram. Technol.*, 6 (2009) 501–512.doi: 10.1111/j.1744-7402.2008.02293.x.

[35] S. P. Victor, W. Paul, V. M. Vineeth, R. Komeri, M. Jayabalan, and C. P. Sharma, "Neodymium doped hydroxyapatite theranostic nanoplatforms for colon specific drug delivery applications," *Colloids Surfaces B Biointerfaces.*, 145 (2016) 539–547.doi: 10.1016/j.colsurfb.2016.05.067.

[36] I. Kostova and M. Traykova, "Cerium (III) and Neodymium (III) Complexes as Scavengers of X / XO- Derived Superoxide Radical," *Medicinal Chemistry.*, 2 (.2006) 463–470.

[37] I. R. De Lima *et al.*, "Understanding the impact of divalent cation substitution on hydroxyapatite: An in vitro multiparametric study on biocompatibility," *J. Biomed. Mater. Res. - Part A*, 98 (2011) 351–358.doi: 10.1002/jbm.a.33126.

[38] H. Shi, Z. Zhou, W. Li, Y. Fan, Z. Li, and J. Wei, "Hydroxyapatite based materials for bone tissue engineering: A brief and comprehensive introduction," *Crystals.*, 11 (2021) 1–18.doi: 10.3390/cryst11020149.